JOURNAL OF Applied Polymer SCIENCE

In vitro Evaluation of Electrospun Gelatin-Bioactive Glass Hybrid Scaffolds for Bone Regeneration

Chunxia Gao,[1] Qiang Gao,[1] Yadong Li,[2] Mohamed N. Rahaman,[3] Akira Teramoto,[1] Koji Abe[1]

[1]Department of Functional Polymer Science, Faculty of Textile Science and Technology, Shinshu University, Ueda 386-8567, Japan
[2]College of Chemistry, Chemical Engineering and Materials Science, Soochow University, Suzhou 215123, People's Republic of China
[3]Department of Materials Science and Engineering, Missouri University of Science and Technology, Rolla, Missouri 65409-0340

Correspondence to: C. Gao (E-mail: s09t155@shinshu-u.ac.jp)

ABSTRACT: Organic–inorganic hybrid materials, composed of phases that interact on a nanoscale and a microstructure that mimics the extracellular matrix, can potentially provide attractive scaffolds for bone regeneration. In the present study, hybrid scaffolds of gelatin and bioactive glass (BG) with a fibrous microstructure were prepared by a combined sol–gel and electrospinning technique and evaluated *in vitro*. Structural and chemical analyses showed that the fibers consisted of gelatin and BG that were covalently linked by 3-glycidoxypropyltrimethoxysilane to form a homogeneous phase. Immersion of the gelatin–BG hybrid scaffolds in a simulated body fluid (SBF) at 37°C resulted in the formation of a hydroxyapatite (HA)-like material on the surface of the fibers within 12 h, showing the bioactivity of the scaffolds. After 5 days in SBF, the surface of the hybrid scaffolds was completely covered with an HA-like layer. The gelatin–BG hybrid scaffolds had a tensile strength of 4.3 ± 1.2 MPa and an elongation to failure of 168 ± 14%, compared to values of 0.5 ± 0.2 MPa and 63 ± 2% for gelatin scaffolds with a similar microstructure. The hybrid scaffolds supported the proliferation of osteoblastic MC3T3-E1 cells, alkaline phosphatase activity, and mineralization during *in vitro* culture, showing their biocompatibility. The results indicate that these gelatin–BG hybrid scaffolds prepared by a combination of sol–gel processing and electrospinning have potential for application in bone regeneration. © 2012 Wiley Periodicals, Inc. J. Appl. Polym. Sci. 000: 000–000, 2012

KEYWORDS: electrospinning; organic–inorganic hybrid scaffolds; gelatin; bioactive glass; sol–gel processing; bone regeneration

Received 17 December 2011; accepted 19 April 2012; published online
DOI: 10.1002/app.37946

INTRODUCTION

Scaffold-based tissue engineering can provide an alternative approach to the use of autogeneic and allogeneic sources to meet the increasing need for implants to repair and regenerate bone. In general, the scaffold should be biocompatible and bioactive, have mechanical properties comparable to the bone to be replaced, and have a porous architecture to support bone ingrowth and integration.[1] A porous architecture that mimics the extracellular matrix (ECM) is desirable; in addition, the scaffolds should have the ability to serve as a temporary support structure to allow cells to synthesize new tissue and to degrade upon neogenesis of tissue.[2–4] The bone ECM consists of an organic–inorganic nanocomposite in which type I collagen fibrils and nanocrystalline hydroxyapatite (HA)-like particles are intimately combined.[5] Biomaterials in the form of nanoparticles, nanofibers, and nanocomposites have been receiving increasing attention for bone repair applications in an attempt to mimic the physical structure of the inorganic HA-like phase of bone.[6–8] In addition, biomaterials have been developed to mimic the collagen fibrils using processing techniques such as electrospinning, phase separation, and self-assembly.[9] The use of electrospinning has been receiving considerable interest as a scaffold fabrication technique because of its ability to create scaffolds with a fibrous architecture that mimics the ECM.[10,11] In addition, electrospinning can be used to process a wide range of materials, does not rely on expensive equipment, and has low operating costs.

In the present study, hybrid scaffolds composed of gelatin and a silicate bioactive glass (BG) were prepared by a combined sol–gel and electrospinning technique. This technique has clear differences from those described in the previous studies. First, the present method relies on the use of a homogeneous solution composed of the polymer (gelatin) and the BG precursor solution, instead of using of discrete phases of the polymer phase and the inorganic phase (typically in the form of particles).[12] Second, the electrospinning technique is used in this study to

create scaffolds with a fine-scale fibrous architecture that mimics the ECM, compared to the coarser architecture produced by the methods used in the previous studies.[13]

Gelatin was selected as the organic phase in the present study because it is a denatured form of collagen, with a composition almost identical to that of collagen. As gelatin is a denatured form of collagen, its use as a scaffold material can avoid the concerns of immunogenicity and pathogen transmission associated with collagen.[14] Electrospun fibrous mats of gelatin have received much attention recently for potential applications in bone regeneration.[15,16] However, most of the reported methods included the use of pungent fluorine-containing reagents. In addition, a crosslinking agent was needed to stabilize the as-prepared structure and to improve the stability of the electrospun gelatin fibers in aqueous media. Although several physical and chemical methods have been used to crosslink gelatin,[17–19] many suffer from drawbacks such as low efficiency and toxicity.

Previous studies have shown the ability to functionalize gelatin using 3-glycidoxypropyltrimethoxysilane (GPTMS), and the use of GPTMS as a coupling agent to covalently link gelatin to silica to form a biocompatible hybrid material.[20–22] However, the hybrid materials in those studies did not have a nanofibrous ECM-like architecture or the silica inorganic phase had limited ability to enhance the bioactivity of the hybrid material. Recently, to improve the bioactivity, the Ca^{2+}-containing gelatin–siloxane fibrous mats were fabricated by sol–gel and electrospinning procedures.[23] However, the effects of immersion time in simulated body fluid (SBF) on the morphology of fibrous mats were not shown. Meanwhile, all Si content in the gelatin–siloxane hybrid was provided by GPTMS. It is difficult to control the Si content and the degree of covalent coupling.[20,24] In our study, changes in the morphology and structure of fibrous mats in an *in vitro* bioactivity test were investigated in detail and ternary silicate BG was chosen as the inorganic phase.

A BG was selected as the inorganic phase in this study because of its attractive bioactive characteristics, such as its conversion to HA, ability to bond to bone and soft tissues, and the ability to support osteogenesis.[25–27] Fibrous composites composed of biodegradable polymers and inorganic particles have been studied recently for applications in bone regeneration.[28] However, most of the composites were prepared by electrospinning mixtures composed of discreet inorganic particles dispersed in a polymer solution.[28,29] Consequently, the fabricated composites suffered from limited interaction between the organic and the inorganic phases which resulted in weak mechanical performance.

The objective of this study was to prepare gelatin–BG hybrid scaffolds by a combined sol–gel and electrospinning technique, and to evaluate the bioactivity, biocompatibility, and mineralization of the scaffolds *in vitro*. A homogeneous solution, composed of gelatin, the BG precursor, and GPTMS as a coupling agent, was used in the electrospinning process to enhance the mixing of the gelatin and BG phases and to covalently link the gelatin and BG at the nanoscale level. We hypothesized that the incorporation of the BG into the gelatin to form a hybrid material would improve the bioactivity and mechanical response of the gelatin, as well as its ability to support the proliferation of osteogenic cells and mineralization *in vitro*. The mechanical response of the hybrid scaffolds was determined in tension, whereas structural and chemical techniques were used to evaluate the bioactivity of the scaffolds in SBF. The biocompatibility of the scaffolds was evaluated from their ability to support the proliferation of osteogenic MC3T3-E1 cells, alkaline phosphatase activity, and mineralization.

MATERIALS AND METHODS

Preparation and Electrospinning of Solutions

The BG composition used in this study, $70SiO_2$–$25CaO$–$5P_2O_5$ (mol %) was the same as that used in a previous study.[30] A precursor solution of the BG composition was prepared by sequentially adding 5 mL tetraethyl orthosilicate, 0.545 mL triethylphosphate, and 1.89 g calcium nitrate tetrahydrate, $Ca(NO_3)_2{\cdot}4H_2O$ (purity, 99%) at 1-h intervals into 32 mL of distilled water containing 16 wt % acetic acid as a catalyst (all chemicals were purchased from Wako Pure Chem. Ind., Japan, and they were used as received unless otherwise stated). The solution was stirred for 24 h at room temperature, aged for 12 h at 40°C, then for 12 h at 60°C, and stored at room temperature for use as described below.

Gelatin (Porcine skin, Type A; Sigma-Aldrich Chemical, Japan) was dissolved in a solvent composed of 60 vol % acetic acid (≥99.7%; Sigma-Aldrich Chemical, Japan) and 40 vol % distilled water, to give a gelatin concentration of 35 wt % (pH = 2.7). The solution was stirred at 50°C for 3 h, after which the BG precursor solution was added. The effective ratio of BG to gelatin in the solution was 30 wt %. After stirring for another 2 h, the required amount of GPTMS (50 wt % based on the weight of gelatin) was added to the gelatin–BG precursor solution, and the system (pH = 3.1) was stirred for 4 h at room temperature before electrospinning.

The main components of the electrospinning apparatus (Kato Tech, Japan) used in this study were a syringe with a flat-end metal needle (1.20 mm internal diameter × 38 mm), a syringe pump for controlling the feeding rate of the solution, a grounded cylindrical stainless steel mandrel, and a high-voltage DC power supply. The solution was electrospun under an applied DC voltage of 12 kV, using a distance of 14 cm between the needle and the collector, and a feeding rate of 1.5 mL/h. The as-prepared gelatin–BG constructs in the shape of thin sheets were heated for 6 h at 110°C with a heating rate of about 1°C/min prior to evaluation. For comparison, electrospun fibers were also prepared from gelatin solutions with or without the coupling agent GPTMS.

Structural and Chemical Characterization of Gelatin–BG Fibrous Scaffolds

The morphology of the electrospun gelatin–BG scaffolds was examined using field-emission scanning electron microscopy (SEM) (Hitachi; S-5000) at an accelerating voltage of 20 kV and a working distance of 14 mm. Conventional transmission electron microscopy (TEM) (JEOL JEM-2010, 120 kV) was used to examine the microstructure of the gelatin–BG fibers. Compositional analysis of the scaffolds was performed using energy-dispersive X-ray (EDS) spectroscopy in the SEM (Hitachi; S-5000) and Fourier transform infrared (FTIR) spectroscopy (IRPrestige-21, Shimadzu, Japan). FTIR was performed in the wavenumber range of 500–4000 cm^{-1}; each FTIR spectrum was obtained from 40 scans at a resolution of 2 cm^{-1}. Measurements were performed in transmission mode using pellets which were pressed from a mixture of 3 mg sample and 197 mg spectroscopic-grade KBr. Wide-angle X-ray diffraction (XRD)

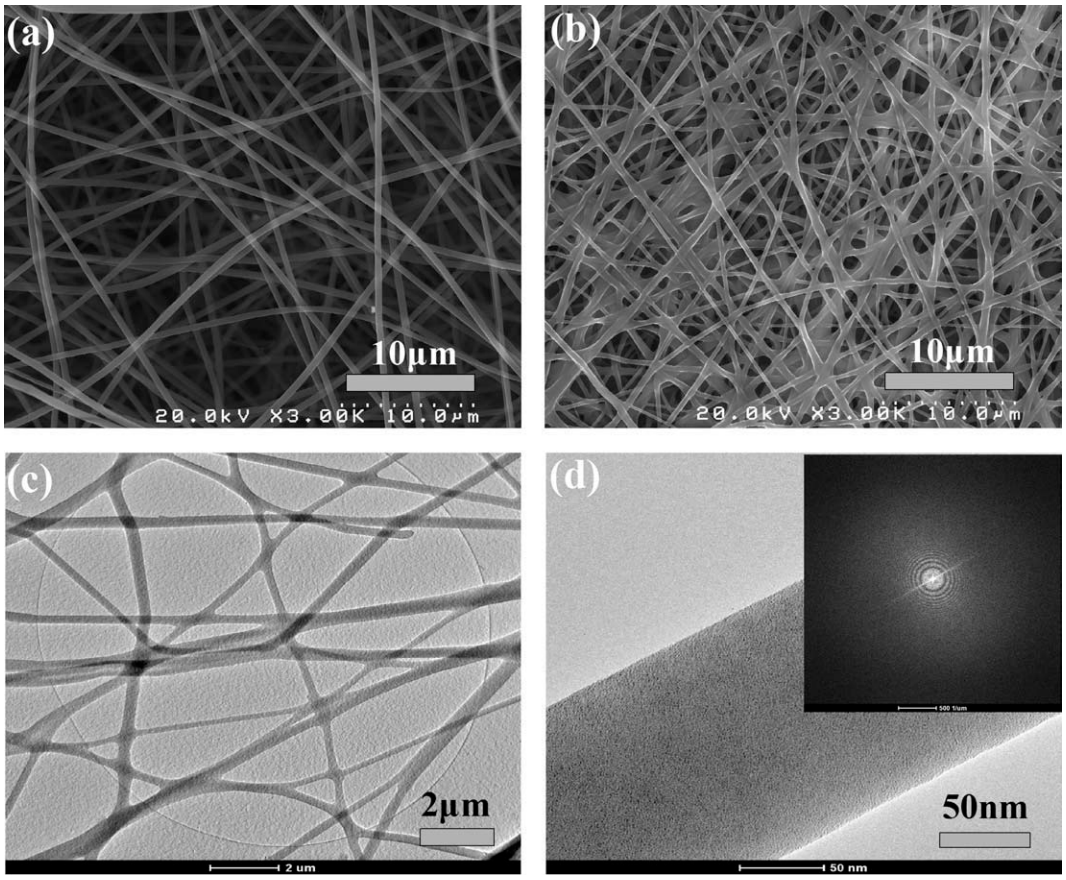

Figure 1. SEM images of electrospun gelatin–BG hybrid scaffolds: (a) as-fabricated, and (b) after immersion in PBS for 12 h; TEM images of as-fabricated gelatin–BG fibers: (c) lower magnification; (d) higher magnification. No particulate phase was observed in the TEM images, whereas the absence of diffraction rings in the SAD image (d, inset) indicated the absence of a crystalline phase.

(Rotorflex RU200B, Rigaku, Japan) was used to determine any crystalline phases present in the gelatin–BG scaffolds; the XRD analysis was performed using Ni-filtered CuK_α radiation ($\lambda = 1.5402$ Å) in a step-scan mode (2°/min) in the 2θ range of 10–60°.

Mechanical Testing

Mechanical testing of electrospun gelatin and gelatin–BG scaffolds was performed in a tensile testing machine (RTC-1250A, A&D, Japan) at a constant deformation rate of 2 mm/min. The specimens were 60 mm long, 5 mm wide, and ~ 10 μm thick, with a gauge length of 40 mm. Prior to testing, the thickness and width of the specimens were measured at three locations along the sample length using a micrometer, and the average values were taken. Ten samples per group were tested.

In Vitro Evaluation of Bioactivity in an SBF

The *in vitro* bioactivity of the electrospun gelatin–BG scaffolds was evaluated from their reaction in SBF. The SBF with a pH of 7.4 was prepared by dissolving reagent-grade NaCl, KCl, $NaHCO_3$, $MgCl_2{\cdot}6H_2O$, $CaCl_2$, and KH_2PO_4 in distilled water at 37°C and buffering with trishydroxymethyl aminomethane and 1*N* HCl solution according to the method described elsewhere.[31] Constructs with the shape of thin disks (22 mm in diameter × ~ 10 μm thick) were placed individually in a static 12-well plate containing 3 mL of SBF per well, and the system was kept at 37°C in 5% CO_2 atmosphere for up to 5 days, with the SBF replaced every 48 h. The samples were removed from the SBF after 12 h, 1 day, 3 days, and 5 days, rinsed three times with distilled water and freeze dried. The morphology, structure, composition, and Ca/P atomic ratio of the samples were investigated using SEM, EDS, and XRD using the procedures described previously.

Cell Culture

The established line of mouse preosteoblastic MC3T3-E1 cells, obtained from the RIKEN Cell Bank (Tsukuba, Japan), were cultured until passage 7 and used in this study. The cells were cultured in α-modified minimum essential medium (α-MEM; GIBCO, Invitrogen Corporation, Grand island, N.Y.), supplemented with 10% heat-inactivated fetal bovine serum (FBS, GIBCO, Invitrogen Corporation, Grand island, N.Y.), 100 U/mL penicillin and 100 U/mL streptomycin. The cultures were incubated at 37°C in a humidified atmosphere containing 5% CO_2, with the medium changed every 48 hours.

Disks (15 mm in diameter × ~ 10 μm thick) were cut from the gelatin–BG and gelatin scaffolds and placed in a 24-well tissue-culture polystyrene (TCP) plate (high-grade polystyrene Nunc™ Dishes, Thermo Fisher Scientific, Denmark). The samples were sterilized in 70% ethanol for 1 h, and then washed three times with sterile phosphate-buffered saline (PBS) for 30 min each to remove residual ethanol. The scaffolds were then immersed in α-MEM overnight under conventional culture conditions. After the culture medium was removed as completely as possible, each

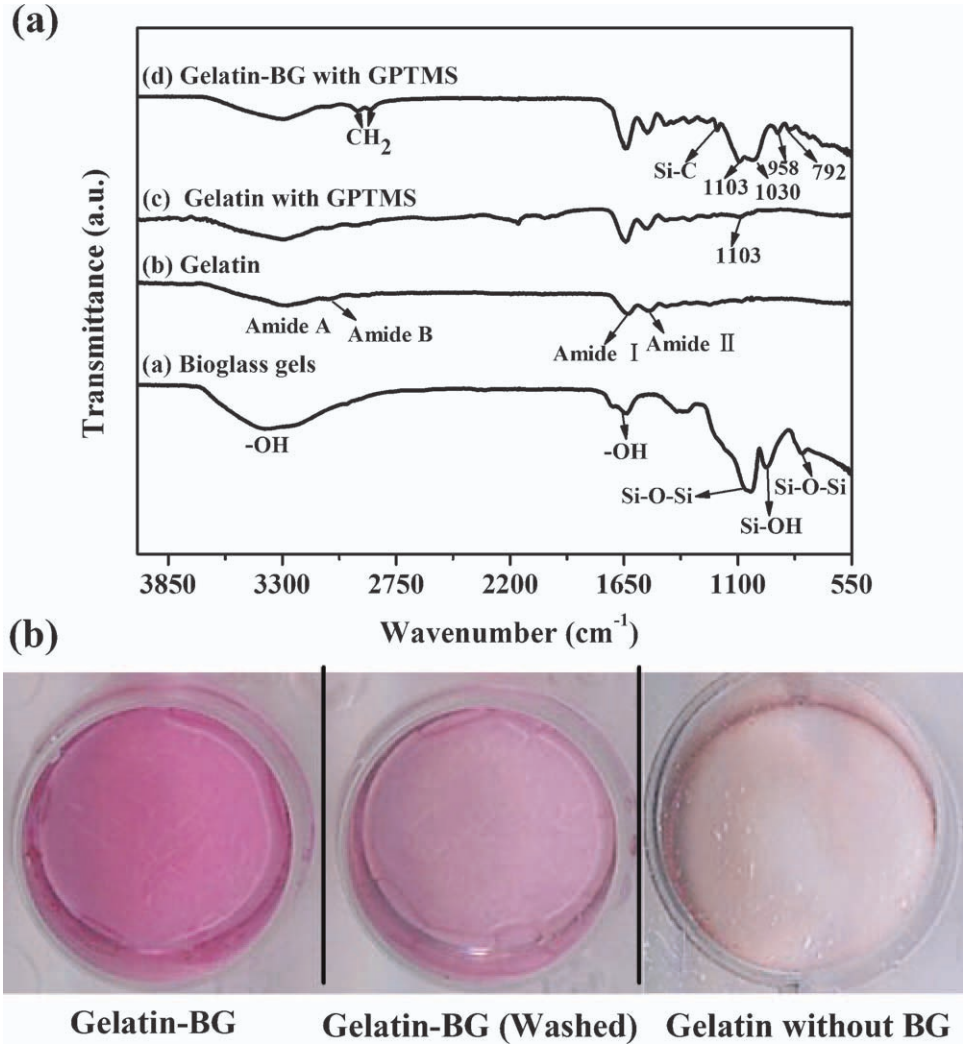

Figure 2. (a) FTIR spectra of BG gel, gelatin fibers, gelatin fibers with GPTMS, and gelatin–BG with GPTMS hybrid scaffolds prepared by electrospinning, (b) optical images of ARS-stained scaffolds of as-fabricated gelatin–BG hybrid, gelatin–BG hybrid after washing with PBS, and gelatin scaffolds. [Color figure can be viewed in the online issue, which is available at wileyonlinelibrary.com.]

scaffold was seeded with cells by adding an MC3T3-E1 cell suspension dropwise onto the scaffolds (1×10^4 cells in 100 μL of medium per well). The cell suspension was fully absorbed, thereby allowing the cells to be distributed within the scaffolds. The cell-seeded scaffolds were incubated for 3 h to allow the cells to adhere to the scaffolds, and additional culture medium was added (1 mL/well). The control group consisted of the same number of cells seeded on TCP substrates.

Morphological Observation of Cultured Cells

After incubation for 1, 3, 7, and 14 days, each scaffold was removed, rinsed three times with PBS, and the cells were fixed with 2.5% glutaraldehyde solution (500 μL/well). After an overnight soak at 4°C, the scaffolds were washed three times with PBS and dehydrated through a graded series of ethanol (50–99%) for 2 min at each concentration. After the final washing with 99% ethanol, the scaffolds were treated three times for 10 min each with *t*-butyl alcohol. Finally, the samples were sputter-coated with gold and observed in an SEM (Hitachi; S-5000) using the conditions described previously.

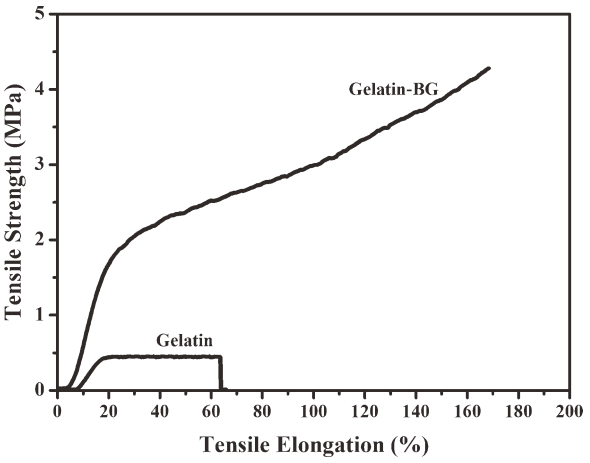

Figure 3. Mechanical response in tension for electrospun scaffolds of (a) gelatin and (b) gelatin–BG hybrid.

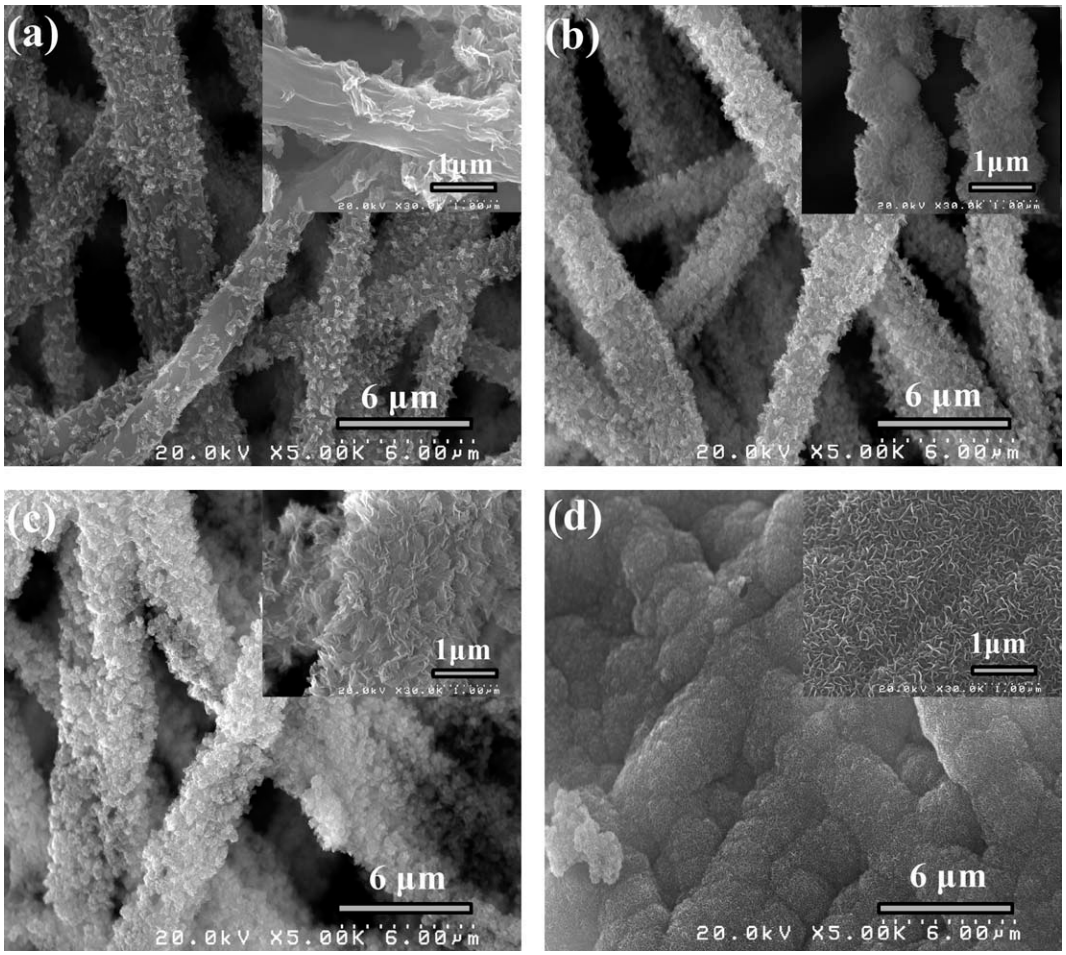

Figure 4. SEM images of electrospun gelatin–BG hybrid scaffolds after immersion in SBF for (a) 12 h, (b) 1 day, (c) 3 days, and (d) 5 days. The inset shows a higher magnification image of the reaction product for each immersion time.

Alkaline Phosphatase Activity

Alkaline phosphatase (ALP) activity of the cell-seeded scaffolds was measured using an alkaline phosphate substrate kit (Wako, Japan). Scaffolds and TCP controls were seeded with MC3T3-E1 cells as described previously, and incubated in α-MEM supplemented with 0.1% β-glycerol phosphate to induce osteoblast differentiation. The ALP activity was measured after incubation times of 3, 5, 7, 14, and 21 days. After each incubation, 500 μL of β-nitrophenyl phosphate solution containing 1 m*M* $MgCl_2$ (Sigma-Aldrich Chemical, Japan) was added and the mixture was incubated for further 10 min at 37°C. The enzymatic reaction was stopped by adding 500 μL of 0.2*N* NaOH, and the absorbance was measured at 405 nm using a microplate reader (Biotrack II; GE Healthcare, Japan).

Alizarin Red S Staining for Mineralization

Alizarin red S (ARS) is a dye that selectively binds to calcium salts and it is widely used for calcium mineral histochemistry.[32] In this study, staining with ARS (Sigma-Aldrich Chemical, Japan) was used to determine the presence of calcium in the as-prepared gelatin–BG hybrids. An ARS staining solution, prepared by mixing 2 g of ARS with 100 mL of water and using dilute ammonium hydroxide to adjust the pH value to 4.0, was added to the as-prepared gelatin–BG scaffolds. A control group, composed of gelatin–BG scaffolds previously washed three times in PBS for 20 min each, was also subjected to the same ARS staining process. After incubation for 10 min at room temperature, the excess dye was removed by washing with deionized water. The gelatin–BG scaffolds were subsequently washed 10 times with deionized water, and examined using an optical microscope (FluoView FV1000, Olympus, Japan); images were taken using a confocal laser scanner (HP Photosmart 3210a All-in-One).

Staining with ARS was also used to detect the matrix mineralization *in vitro*. After incubation for 14 days, the cell-seeded scaffolds were washed three times with PBS, fixed with 10% formaldehyde for 1 h, and then rinsed five times for 5 min each with deionized water. After adding the ARS stain, each well was incubated for 10 min at room temperature, and examined using the same procedure described above.

Statistical Analysis

All biological experiments (three samples in each group) were run in triplicate. The data are presented as the mean ± standard deviation (SD). Statistical analysis was performed using one-way analysis of variance with the level of significance set at $p < 0.05$.

Applied Polymer SCIENCE

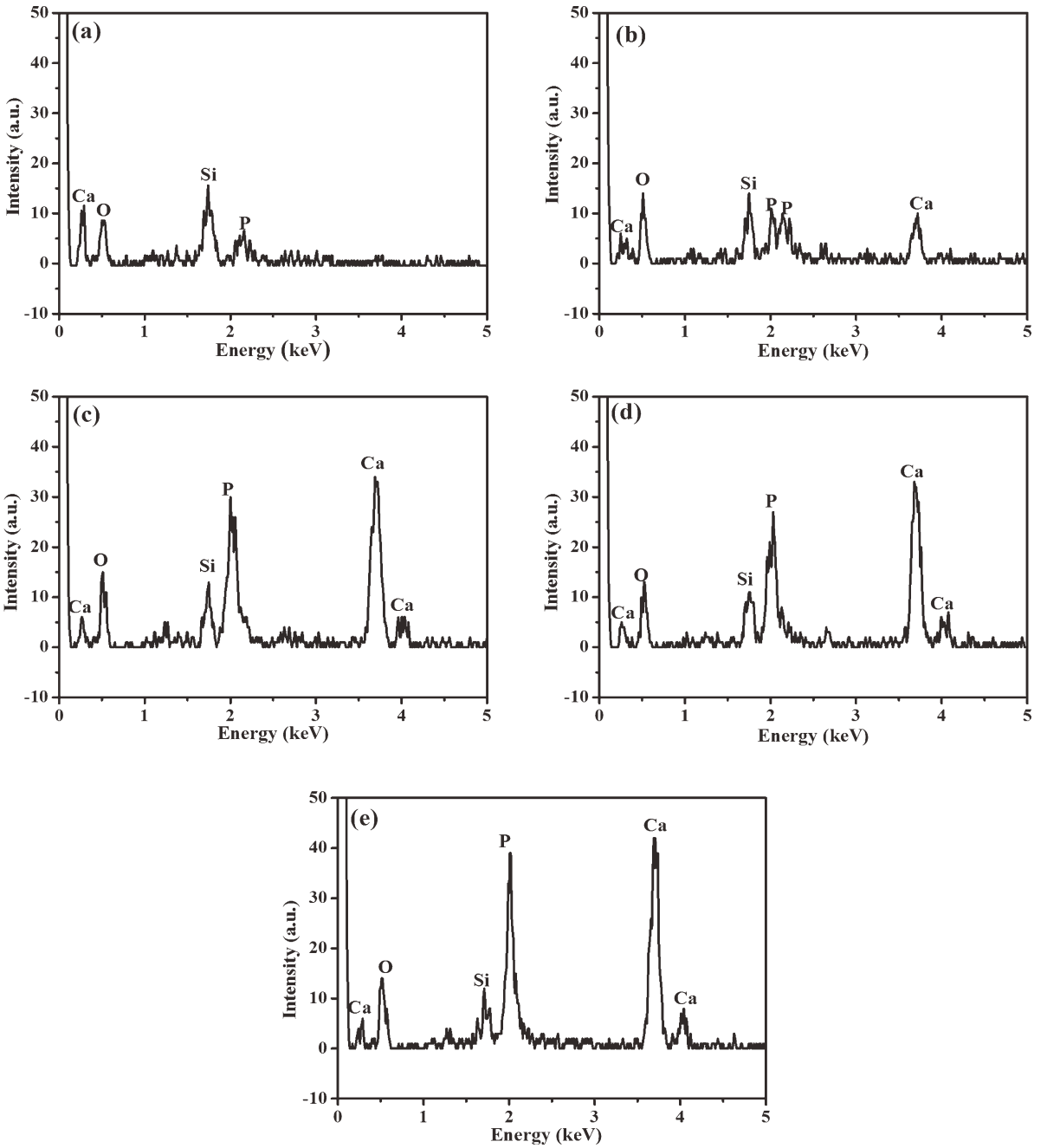

Figure 5. EDS spectra of electrospun gelatin–BG hybrid scaffolds as-prepared (a), and after immersion in SBF for 12 h (b); 1 day (c), 3 days (d), and 5 days (e).

RESULTS

Structural and Chemical Characteristics of Electrospun Gelatin–BG Scaffolds

SEM showed that the as-prepared gelatin–BG scaffolds covalently linked by GPTMS were composed of randomly distributed fibers with a uniform diameter, which were free from bead-like defects [Figure 1(a)]. After immersion for 12 h in PBS, the fiber diameter appeared to increase slightly [Figure 1(b)], presumably as a result of swelling, but the scaffold maintained the porous fibrous architecture. TEM of the gelatin–BG fibers [Figure 1(c)] showed a smooth surface and a homogeneous single-phase material. Higher resolution TEM [Figure 1(d)] did not show a particulate phase or a crystalline phase, a finding that was confirmed by selected area diffraction (SAD) [Figure 1(d), inset]. Therefore, within the limits of resolution of the TEM, the fibers consisted of an amorphous single-phase material. The average fiber diameter of the electrospun gelatin–BG scaffolds, determined from more than 100 randomly selected fibers using the Image J software, was 192 ± 8 nm.

Figure 2(a) shows FTIR spectra of the as-prepared gelatin–BG hybrids and gelatin fibers that contained the coupling agent GPTMS. For comparison, the FTIR spectra of the pure gelatin

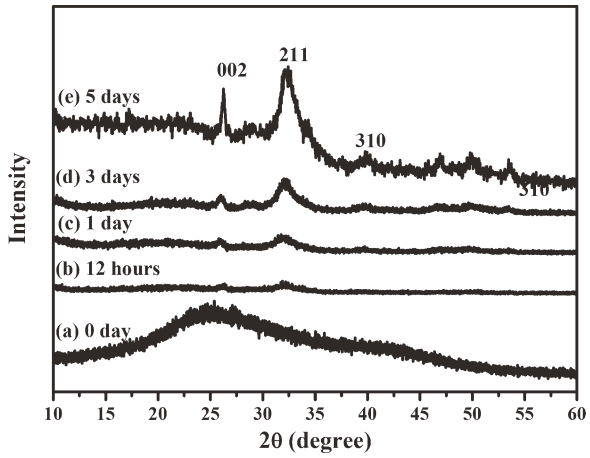

Figure 6. XRD patterns of electrospun gelatin–BG hybrid scaffolds as-prepared and after immersion in SBF for the times shown.

fibers without GPTMS and the BG gel are also shown for reference. The main characteristic resonances of pure gelatin and BG gel also appeared in the spectra of gelatin–BG hybrids: at 1560 cm^{-1} attributed to the N—H bending vibration in the amide II, at 1670 cm^{-1} attributed to the C=O stretching vibration in the amide I, at 2952 cm^{-1} attributed to the C—H bending vibration for the amide B, and at 3310 cm^{-1} attributed to N—H vibration for amide A.[22] In addition, the characteristic resonances of BG include those at 792 cm^{-1} attributed to the Si—O—Si symmetric stretching, at 1000–1110 cm^{-1} attributed to the Si—O—Si asymmetric stretching, and at 958 cm^{-1} attributed to the Si—OH asymmetric stretching.[33]

Compared with the spectra of the BG gel, the resonance at 958 cm^{-1} became weak in the gelatin–BG hybrid owing to the reduction in the number of Si—OH groups, indicating the enhanced formation of the silica network.[33] Moreover, the resonances at 1030 and 1103 cm^{-1} in the gelatin–BG hybrid were attributed to the Si—O—Si asymmetric stretching [Figure 2(a)], confirming the formation of the silica network. The same phenomenon observed in the gelatin–GPTMS system indicated that the silane end of GPTMS has taken part in the formation of this silica network.[34–36] An additional resonance in the spectrum of the gelatin–BG fibers corresponding to Si—C stretching was found at 1235 cm^{-1}.[35] Combined with weak resonances appeared at 2942 and 2862 cm^{-1}, attributed to CH_2 stretching vibrations, presumably resulting from methyl groups of GPTMS, indicated the presence of GPTMS in the gelatin–BG hybrid.[23,35]

As described previously, ARS staining was used to characterize the presence of calcium in the gelatin–BG hybrids. Figure 2(b) shows images of ARS-stained gelatin–BG hybrids as-prepared and after washing with PBS, and gelatin scaffolds (without BG). The large difference in red color between the as-prepared gelatin–BG hybrids and the gelatin (without BG) indicated the presence of calcium in the as-prepared hybrid material.[22,32] After washing the as-prepared gelatin–BG hybrid with PBS (three times for 20 min each), the red stain had a lower intensity but it was still clearly present [Figure 2(b)], indicating the presence of calcium in the gelatin–BG hybrid scaffold even after the prolonged washing process.

Mechanical Properties

Figure 3 shows the mechanical response in tension of the gelatin and gelatin–BG hybrid scaffolds prepared by the electrospinning process. For both materials, the stress initially increased more rapidly and almost linearly with the elongation, but the stress at any elongation was far higher for the hybrid scaffolds. Subsequently, for the gelatin scaffold, the stress showed little increase with elongation until failure; in the case of the gelatin–BG hybrid, the stress continued to increase with elongation until failure. The tensile strength of the gelatin scaffolds was 0.5 ± 0.2 MPa and the elongation to failure was 63 ± 2%. In comparison, the gelatin–BG scaffolds had a tensile strength of 4.3 ± 1.2 MPa and an elongation to failure of 168 ± 14%.

In Vitro Bioactivity

The surface of the electrospun gelatin–BG hybrid scaffolds showed considerable morphological changes after immersion in SBF (Figure 4). Many fine, needle-like particles were formed homogeneously on the surface of the fibers within 12 h [Figure 4(a)], and they appeared to be well attached to the surface [Figure 4(a), inset]. The size and number of these needle-like particles increased with immersion time. After 1 day, the surface of the fibers was almost completely covered with fine particles, but the porous and fibrous architecture of the scaffold was still evident [Figure 4(b)]. The particles increased in size and showed a more rounded morphology after 3 days. After immersion for 5 days, the surface of the scaffold was almost completely covered with a layer of reaction product, and the porous fibrous architecture of the scaffold was no longer visible [Figure 4(d)]; the surface of the reaction product consisted of fine, needle-like particles [Figure 4(d), inset].

EDS analysis showed that when compared to the as-prepared gelatin–BG scaffolds [Figure 5(a)], immersion in SBF for 12 h resulted in an increase in the intensity (height) of both the Ca and the P peaks, and a decrease in the Si peak intensity [Figure 5(b)]. The intensities of the Ca and P peaks continued to increase with longer immersion time [Figure 5(c–e)]; in addition, a small Si peak was still present.

XRD analysis of the as-prepared gelatin–BG hybrid scaffold did not show any measurable diffraction peaks (Figure 6), indicating an amorphous material. This finding is in agreement with the TEM observation described previously [Figure 1(d)]. However, after immersion of the scaffold for 12 h in SBF, small peaks were detected at 26 and 32°, which corresponded to the dominant (002) and (211) reflection planes in a reference HA (JCPDS 72-1243). The intensity of these two peaks increased with immersion time (up to 5 days used in this study). Taken together, the EDS and XRD analyses indicated the formation of an HA-like reaction product on the surface of the gelatin–BG scaffold within 12 h of immersion in SBF which increased with immersion time.

SEM images show the morphology and density of MC3T3-E1 cells cultured for 3, 7, and 14 days on the gelatin–BG hybrids [Figure 7(a)] and on the gelatin scaffolds (control) [Figure 7(b)]. For both scaffolds, the cells showed an increase in density with increasing incubation time. However, differences in morphology were also apparent between the cells cultured on the

Applied Polymer SCIENCE

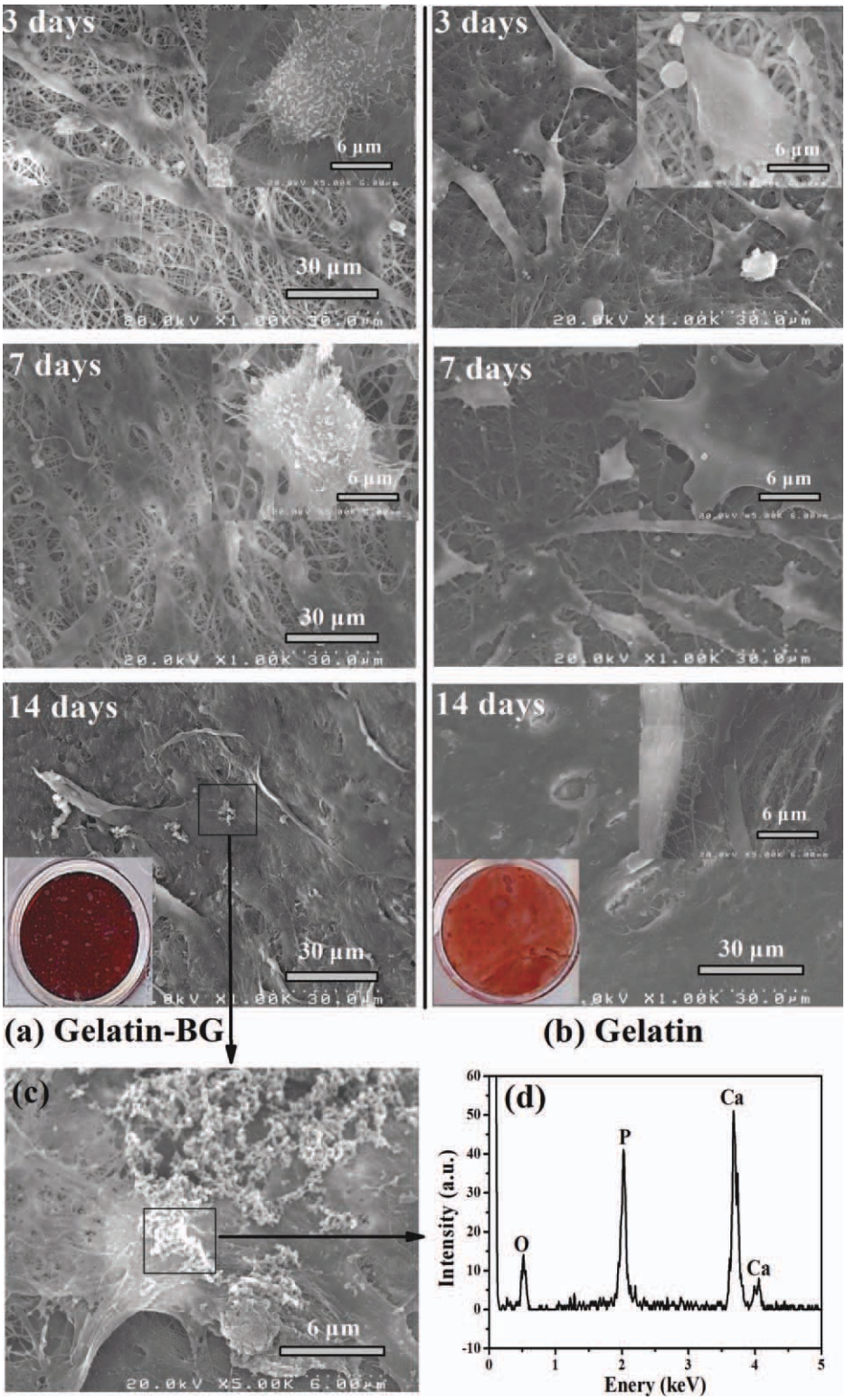

Figure 7. SEM images of MC3TC-E1 cell morphology on (a) gelatin–BG hybrid scaffolds and (b) gelatin scaffolds, after incubation for the times shown; (c) SEM image of gelatin–BG hybrid scaffolds after incubation for14 days at higher magnification; (d) EDS analysis of the nodules formed after incubation for 14 days. [Color figure can be viewed in the online issue, which is available at wileyonlinelibrary.com.]

gelatin–BG scaffold and the gelatin scaffold. After incubation for 3 days, the cells appeared to be well attached to the surface of both scaffolds, and they presented a characteristic polygonal morphology. After 7 days, some particles could be found on the surface of the gelatin–BG scaffolds, whereas the surface of the cells cultured on the gelatin scaffolds was smooth. After 14 days

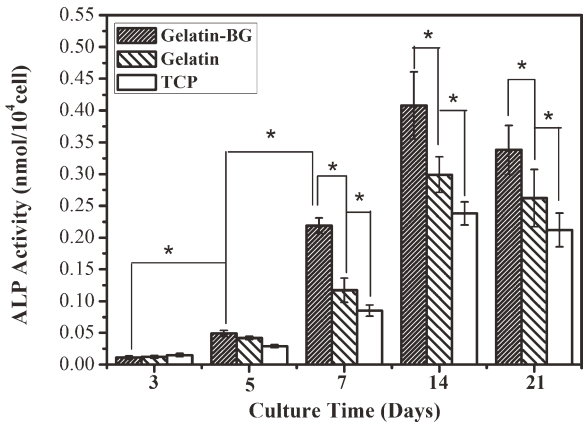

Figure 8. ALP activity of gelatin–BG hybrid scaffolds, gelatin scaffolds, and TCP control substrates seeded with MC3T3-E1 cells and incubated for 3, 5, 7, 14, and 21 days. Mean ± SD; *significant difference between pairs ($P < 0.05$).

of culture, the surface of the gelatin–BG scaffold was covered with multicellular layers, associated with some small spherical structures and nodules on the surface of the cellular layer.

SEM at higher magnification [Figure 7(c)] showed the morphology of the deposited nodules on the cellular surface of the gelatin–BG scaffolds after 14 days, whereas EDS analysis [Figure 7(d)] showed that the nodules were composed of a calcium phosphate material with Ca/P atomic ratio of 1.39. In addition, ARS staining was used to evaluate the ability of the cell-seeded gelatin–BG scaffolds to support mineralization after an incubation time of 14 days [Figure 7(a,b), inset]. Both scaffolds showed a bright red staining, indicating the presence of calcium. However, the greater intensity of the red stain indicated a greater ability of the gelatin–BG hybrids to support mineralization and formation of nodules.

ALP Activity

Results of spectrophotometric measurement of ALP activity of MC3T3-E1 cells cultured on the gelatin–BG scaffolds, gelatin scaffolds, and TCP controls for 3, 5, 7, 14, and 21 days are shown in Figure 8. As shown, the ALP activity increased with time, indicating that the MC3T3-E1 cells were able to carry out an osteogenic function on the gelatin–BG and gelatin scaffolds. However, the ALP activity of the cells cultured on the gelatin–BG scaffolds was higher than that for cells cultured on the gelatin scaffolds and TCP at 7, 14, and 21 days. This higher ALP activity showed that the gelatin–BG scaffolds had a greater capacity to support mineralization after incubation times of 7 days or longer when compared to the gelatin scaffolds and TCP control substrates.

DISCUSSION

The results show that gelatin–BG hybrid scaffolds prepared in this study by a combined sol–gel and electrospinning technique have desirable characteristics for potential application in bone repair. The scaffolds have a fibrous architecture that mimics the ECM, are bioactive, and support the proliferation of osteoblastic MC3T3-E1 cells, ALP activity, and mineralization *in vitro*.

SEM and TEM showed that the gelatin–BG scaffolds had a porous architecture consisting of fibers with a nearly uniform diameter of ~ 200 nm (Figure 1). Furthermore, the fibers in the as-prepared scaffolds were amorphous, as determined by XRD and SAD in the TEM, and they consisted of a homogeneous phase within the limits of resolution of the TEM (Figures 1 and 6). These results indicate that the fibers consist of a hybrid network in which gelatin polymers and presumably siloxane (Si—O—Si) chains present in the sol–gel-derived BG precursor solution are covalently linked by GPTMS to form a homogenous phase.

It is well known that acid-catalyzed hydrolysis and condensation reactions in solution sol–gel processing of inorganic silicates lead to the formation of a siloxane (Si—O—Si) network. FTIR analysis confirmed the presence of amide bands of gelatin, (Si—O—Si) groups of BG in the as-prepared gelatin–BG scaffolds (Figure 2). Meanwhile, the FTIR analysis also showed the presence of GPTMS in the spectrum of the gelatin–BG hybrid scaffolds. Presumably, the silane end of GPTMS has taken part in the formation of the silica network.

The incorporation of calcium and phosphate ions into the as-prepared gelatin–BG hybrid was shown using ARS staining and EDX analysis.[22,37] The rapid mineralization in SBF also indicated the presence of calcium in the as-prepared gelatin–BG hybrid (Figures 4 and 5). However, the incorporation of calcium in the hybrid scaffolds is unclear. Although some previous studies have indicated the incorporation of calcium in gelatin–siloxane hybrids,[38] other studies have indicated that the incorporation of calcium in gelatin–silica hybrids was difficult.[39] Further study is being performed to more clearly determine the presence of calcium in the hybrid scaffolds prepared in this study.

A schematic diagram summarizing the main steps in the formation of the gelatin−BG hybrid fibers is shown schematically in Figure 9. Initially, hydrolysis and partial condensation of the BG precursor solution under acidic conditions presumably resulted in the formation of a siloxane network in which the Ca and P are incorporated into the network in the same proportions as the starting solution [Figure 9(a)]. After addition of the sol–gel-derived BG solution to the gelatin solution and homogenization of the mixture by stirring, addition of GPTMS to the mixture resulted presumably in ring-opening reactions in the epoxy groups.[40] The protonated epoxy group is believed to attack nucleophilic groups such as —NH_2, and —COOH on the amino acid residues of the gelatin chains, resulting in the bonding of GPTMS molecules to the gelatin chains [Figure 9(b)].[41] Simultaneously, the methoxysilane groups (Si—OCH_3) of GPTMS are hydrolyzed to give silanol (Si—OH) groups. This mixture was used in the electrospinning step to prepare the fibrous scaffolds. Heating the electrospun constructs to 110°C resulted presumably in a silica network by condensation between the hydroxyl groups of the GPTMS and the siloxane chains, to give a covalently bonded network of gelatin and siloxane chains [Figure 9(c)].

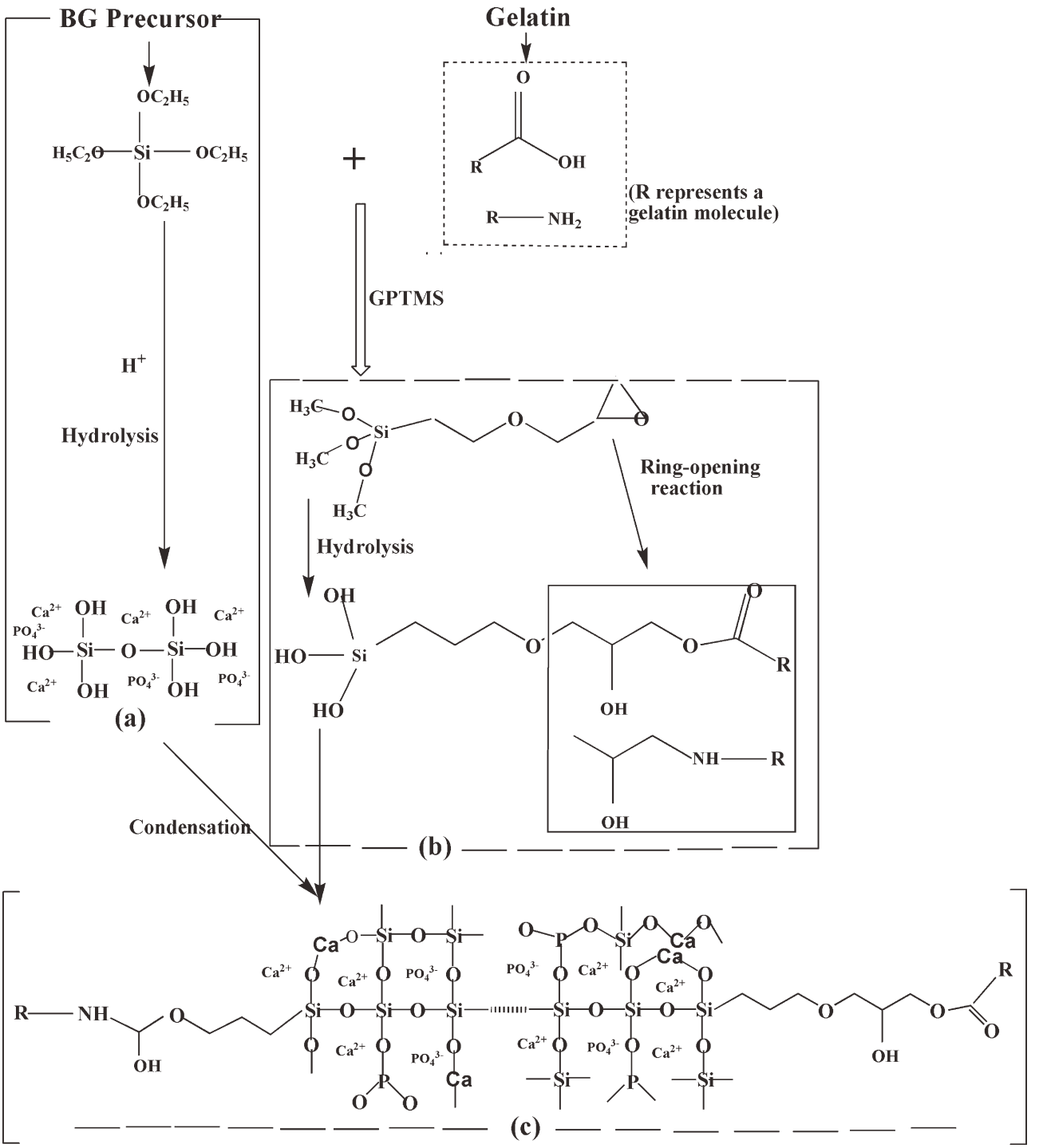

Figure 9. Schematic representation of the formation of electrospun gelatin–BG hybrids composed of gelatin polymers bonded to siloxane chains of sol–gel-derived BG using a coupling agent (GPTMS).

An interesting feature of the results is the rapid formation of HA-like precipitates within 12 h of immersion in SBF; these precipitates formed an HA-like layer on the gelatin–BG scaffolds after 5 days (Figures 4–6). The formation of an HA-like layer on the surface of a scaffold is desirable for bone repair because it has been shown to be responsible for producing a firm bond between the scaffold and bone as well as soft tissues *in vivo*.[26] In comparison, the formation of an HA-like layer was observed after 21 days for gelatin–apatite composite[42] and after 7 days for gelatin–siloxane fibrous mats.[23] The rapid formation of an HA-like material on the gelatin−BG scaffolds prepared in this study presumably resulted from (1) rapid degradation of the scaffolds resulting from the fine diameter of the electrospun fibers and (2) the uniform mixing of the gelatin and siloxane

network. The rate of dissolution of a material depends inversely on the radius. Consequently, these electrospun gelatin−BG scaffolds should have a high dissolution rate, leading to rapid release of calcium ions and precipitation of an HA-like material. The uniform mixing of the gelatin and siloxane network can lead to numerous nucleation sites for the HA-like material to nucleate and grow. In an aqueous phosphate solution, such as an SBF, silicon ions can form silanol groups on the surface of the gelatin−BG fibers which are believed to act as nucleation sites for the formation of HA crystals.[43]

In addition to enhancing the bioactivity, the incorporation of BG into the gelatin system also enhanced the mechanical response. Both the tensile strength and the elongation to failure of the gelatin–BG hybrids were superior to those of the gelatin material with a similar architecture. Presumably, the homogeneously distributed inorganic siloxane network covalently bonded to the gelatin enabled the hybrid nanofibers to better resist extension in response to an applied load. In addition to the higher tensile strength, the ability to maintain a high ductility (elongation to failure) should be beneficial for the potential use of these gelatin–BG hybrids as a membrane or scaffold for bone regeneration.

In vitro cell-culture studies confirmed that the gelatin–BG hybrid scaffolds prepared in this work were biocompatible. The scaffolds supported the attachment and proliferation of osteogenic MC3T3-E1 cells (Figure 7) and mineralization of the cell-seeded scaffolds (Figure 7, inset). In addition, the cell-seeded scaffolds showed a greater capacity to support ALP activity when compared to control substrates (cell-seeded gelatin scaffold and TCP) (Figure 8). Research is presently underway to evaluate the ability of these gelatin–BG scaffolds to support bone regeneration *in vivo*.

CONCLUSIONS

A process that combined sol−gel and electrospinning techniques was used to prepare gelatin–BG hybrid scaffolds with a fibrous architecture that mimicked the ECM. The scaffolds consisted of an amorphous homogenous phase consisting of gelatin covalently bonded to a siloxane network. Immersion of the scaffolds in an SBF resulted in the formation of HA-like crystals on the surface of the fibers within 12 h, showing the excellent bioactivity of the scaffolds. The external surface of the scaffolds was almost completely covered with an HA-like layer within 5 days. The gelatin–BG hybrid scaffolds supported the proliferation of osteoblastic MC3T3-E1 cells, ALP activity, and mineralization during *in vitro* culture, showing their biocompatibility. When compared to electrospun gelatin scaffolds with the same nanofibrous architecture, the gelatin–BG hybrid scaffolds showed approximately an order of magnitude increase in tensile strength (from 0.5 ± 0.2 to 4.3 ± 1.2 MPa) and a large improvement in the elongation to failure (from 63 ± 2 to 168 ± 14%). The results indicate that these gelatin−BG hybrids have potential for application as scaffolds in bone regeneration.

ACKNOWLEDGMENTS

This study was financially supported by a Grant-in-Aid for Global COE program by the Ministry of Education, Culture, Sports, Science and Technology of Japan.

REFERENCES

1. Hutmacher, D. W. *Biomaterials* **2000,** *21*, 2529.
2. Alves, N. M.; Leonor, I. B.; Azevedo, H. S.; Reis, R. L.; Mano, J. F. *J. Mater. Chem.* **2010,** *20*, 2911.
3. Tanase, C. E.; Popa, M. I.; Verestiuc, L. *Mater. Lett.* **2011,** *65*, 1681.
4. Mata, A.; Geng, Y.; Henrikson, K. J.; Aparicio, C.; Stock, S. R.; Satcher, R. L.; Stupp, S. *Biomaterials* **2010,** *31*, 6004.
5. Venugopal, J.; Low, S.; Choon, A. T.; Kumar, T. S. S.; Ramakrishna, S. *J. Mater. Sci. Mater. Med.* **2008,** *19*, 2039.
6. Tilocca, A. *J. Mater. Chem.* **2011,** *21*, 12660.
7. Holzwarth, J. M.; Ma, P. X. *Biomaterials* **2011,** *32*, 9622.
8. Calandrelli, L.; Annunziata, M.; Ragione, F. D.; Laurienzo, P.; Malinconico, M.; Oliva, A. *J. Mater. Sci. Mater. Med.* **2010,** *21*, 2923.
9. Wei, G. B.; Ma P. X. *Adv. Funct. Mater.* **2008,** *18*, 3568.
10. Teo, W. E.; Ramakrishna, S. *Compos. Sci. Technol.* **2009,** *69*, 1804.
11. Jang, J. H.; Castano, O.; Kim, H. W. *Adv. Drug. Deliv. Rev.* **2009,** *61*, 1065.
12. Mozafari, M.; Rabiee, M.; Azami, M.; Maleknia, S. *Appl. Surf. Sci.* **2010,** *257*, 1740.
13. Liu, X. H.; Smith, L. A.; Hu, J.; Ma, P. X. *Biomaterials* **2009,** *30*, 2252.
14. Ross-Murphy, S. B. *Polymer* **1992,** *33*, 2622.
15. Choktaweesap, N.; Arayanarakul, K.; Aht-ong, D.; Meechaisue, C.; Supaphol, P. *Polym. J.* **2007,** *39*, 622.
16. Chen, H. C.; Jao, W. C.; Yang, M. C. *Polym. Adv. Technol.* **2009,** *20*, 98.
17. Zhang, Y. Z.; Venugopal, J.; Huang, Z. M.; Lim, C. T.; Ramakrishna, S. *Polymer* **2006,** *47*, 2911.
18. Ko, J. H.; Yin, H. Y.; An, J.; Chung, D. *J. Macromol. Res.* **2010,** *18*, 137.
19. Panzavolta, S.; Gioffre, M.; Focarete, M. L.; Gualandi, C.; Foroni, L. *Acta Biomater.* **2011,** *7*, 1702.
20. Mahony, O.; Tsigkou, O.; Ionescu, C.; Minelli, C.; Ling, L.; Hanly, R.; Smith, M. E.; Stevens, M, M.; Jones, J. R. *Adv. Funct. Mater.* **2010,** *20*, 3835.
21. Ren, L.; Tsuru, K.; Hayakawa, S.; Osaka, A. *J. Sol. Gel Sci. Technol.* **2003,** *26*, 1137.
22. Song, J. H.; Yoon, B. H.; Kim, H. E.; Kim, H. W. *J. Biomed. Mater. Res. A* **2008,** *84*, 875.
23. Ren, L.; Wang, J.; Yang, F. Y.; Wang, L.; Wang, D.; Wang, T. X.; Tian, M. M. *Mater. Sci. Eng.* **2010,** *30*, 437.
24. Poologasundarampillai, G.; Yu, B.; Tsigkou, O.; Valliant, E.; Yue, S.; Lee, P. D.; Hamilton, R. W.; Stevens, M. M.; Kasuga, T.; Jones, J. R. *Soft Matter* **2012,** *8*, 4822.
25. Allo, B. A.; Rizkalla, A. S.; Mequanint, K. *Langmuir* **2010,** *26*, 18340.
26. Hench, L. L. *J. Am. Ceram. Soc.* **1998,** *81*, 1705.
27. Rahaman, M. N.; Day, D. E.; Bal, B. S.; Fu, Q.; Jung, S. B.; Bonewald, L. F. *Acta Biomater.* **2011,** *7*, 2355.

28. Fujihara, K.; Kotaki, M.; Ramakrishna, S. *Biomaterials* **2005,** *26*, 4139.
29. Sheikh, F. A.; Barakat, N. A. M.; Kanjwal, M. A.; Park, S. J.; Park, D. K.; Kim, H. Y. *Macromol. Res.* **2010,** *18*, 59.
30. Choi, J. Y.; Lee, H. H.; Kim, H. W. *J. Mater. Sci. Mater. Med.* **2008,** *19*, 3287.
31. Kokubo, T.; Takadama, H. *Biomaterials* **2006,** *27*, 2907.
32. Gregory, C. A. *Anal. Biochem.* **2004,** *329*, 77.
33. Duran, A.; Serna, C.; Fornes, V.; Navarro, J. M. F. *J. Non-Cryst. Solids* **1986,** *82*, 69.
34. Tonda-Turo, C.; Gentile, P.; Saracino, S.; Chiono, V.; Nandagiri, V. K.; Muzio, G.; Canuto, R. A.; Ciardelli, G. *Int. J. Biol. Macromol.* **2011,** *49*, 700.
35. Chernev, G. E.; Borisova, B. V.; Kabaivanova, L. V.; Salvado, I. M. *Cent. Eur. J. Chem.* **2010,** *8*, 870.
36. Liu, Y. L.; Su, Y. H.; Lai, J. Y. *Polymer* **2004,** *45*, 6831.
37. Toworfe, G. K.; Composto, R. J.; Shapiro, I. M.; Ducheyne, P. *Biomaterials* **2006,** *27*, 631.
38. Ren, L.; Tsuru, K.; Hayakawa, S.; Osaka, A. *Biomaterials* **2002,** *23*, 4765.
39. Lin, S.; Ionescu, C.; Pike, K. J.; Smith, M. E.; Jones, J. R. *J. Mater. Chem.* **2009,** *19*, 1276.
40. Ren, L.; Tsuru, K.; Hayakawa, S.; OsakaA. *J. Sol. Gel Sci. Technol.* **2001,** *2*, 115.
41. Schottner, G. *Chem. Mater.* **2001,** *13*, 3422.
42. Liu, X.; Smith, L. A.; Hu, J.; Ma, P. X. *Biomaterials* **2009,** *30*, 2252.
43. Cui, W.; Li, X.; Xie, C.; Zhuang, H.; Zhou, S.; Weng, J. *Biomaterials* **2010,** *31*, 4620.